Ferromagnetic nematic suspensions with negative dielectric anisotropy: Competing effects of magnetic and electric fields

Shivaraja Santhegudda Jayaramappa,[1,*] Anaswara Das Kunnummal,[1,*] Ramesh Manda,[1] Alenka Mertelj,[2] Darja Lisjak,[3] and Surajit Dhara[1,†]

[1] *School of Physics, University of Hyderabad, Hyderabad 500046, India*

[2] *Department of Complex Matter, Jozef Stefan Institute, Jamova cesta 39, Ljubljana SI-1000, Slovenia*

[3] *Department for Materials Synthesis, Jozef Stefan Institute, Jamova cesta 39, Ljubljana SI-1000, Slovenia*

(Received 2 December 2024; revised 15 April 2025; accepted 25 April 2025; published 14 May 2025)

The successful development of ferromagnetic nematic liquid crystals (FNLCs) has opened up a new direction for research in liquid crystals, which has the potential for technological applications. Previous research has predominantly focused on FNLCs based on positive dielectric anisotropy liquid crystals. In this paper, we report the preparation and comprehensive characterization of an FNLC with low birefringence and negative dielectric anisotropy. The suspension was prepared by dispersing and stabilizing barium hexaferrite nanoplatelets in the nematic liquid crystal. The suspension exhibits superior magnetocapacitance and magnetoviscous effects compared with conventional isotropic ferrofluids. We show that electric and magnetic fields applied simultaneously perpendicular to the director have competing effects on the director's alignment and the nanoplatelets' magnetic moments. This ferromagnetic nematic suspension broadens the scope of fundamental studies and has the potential for applications in magnetoelectric and magneto-optic sensors.

DOI: 10.1103/PhysRevApplied.23.054040

I. INTRODUCTION

Liquid crystals (LCs) are partially ordered fluids made of shape-anisotropic organic molecules [1]. The molecules have a rigid core connected to flexible alkyl chains [2]. The core part of the molecules is made mainly of benzene rings; hence, liquid crystals are diamagnetic materials [1,3]. Since the diamagnetic susceptibility is very small ($\Delta\chi \approx 10^{-6}$), a strong magnetic field (approximately 1 T) is required to reorient the director (the average direction of molecular alignment) along the magnetic field, which is crucial for applications. Such a high magnetic field is difficult to achieve for device applications, and this prevents the liquid crystals from being used in magneto-optic devices.

The discovery of ferromagnetic suspension by dispersing monodomain ferromagnetic nanoplatelets in ordinary diamagnetic liquid crystals has not only expanded the scope of liquid crystals for fundamental studies but also opened possibilities for new applications [4–12]. The direction of the magnetic moment of the nanoplatelets is perpendicular to their plane. The LC molecules are anchored orthogonal to the nanoplatelets due to the surfactant molecules. This results in an effective coupling between the nematic director and the magnetic moment of the platelets, causing them to preferentially align in the same direction, as shown in Fig. 1(b) [4,13]. A small concentration of ferromagnetic particles does not appreciably affect the long-range orientational order of the molecules, but the suspensions become ferromagnetic, showing a giant response at small magnetic fields (< 10 mT). Hence, ferromagnetic nematic suspensions have drawn attention for possible device applications [14–17]. So far, cyanobiphenyl-based compounds such as 5CB (4-Cyano-4′-pentylbiphenyl), 8CB (4′-Octyl-4-biphenylcarbonitrile), and E7 (nematic mixture) with longitudinal -CN groups have been used for preparing such ferromagnetic suspensions [18]. These materials have a large positive dielectric anisotropy and moderate birefringence. In the previously mentioned suspensions, both the magnetic and electric fields have a synergistic aligning effect when simultaneously applied perpendicular to the director, i.e., the electric and magnetic fields both tend to align the director in the field direction.

To enhance the scope of fundamental studies and possible applications, suspensions with negative dielectric anisotropy are desirable. In such suspensions, the simultaneous electric field and magnetic field will have an antagonistic aligning effect, i.e., the director would tend to reorient parallel to the magnetic field or perpendicular to the electric field depending on the competing effects of the magnetic and electric torques. Here, we report the preparation of a ferromagnetic nematic suspension by

*These authors contributed equally to this work.
†Contact author: surajit@uohyd.ac.in

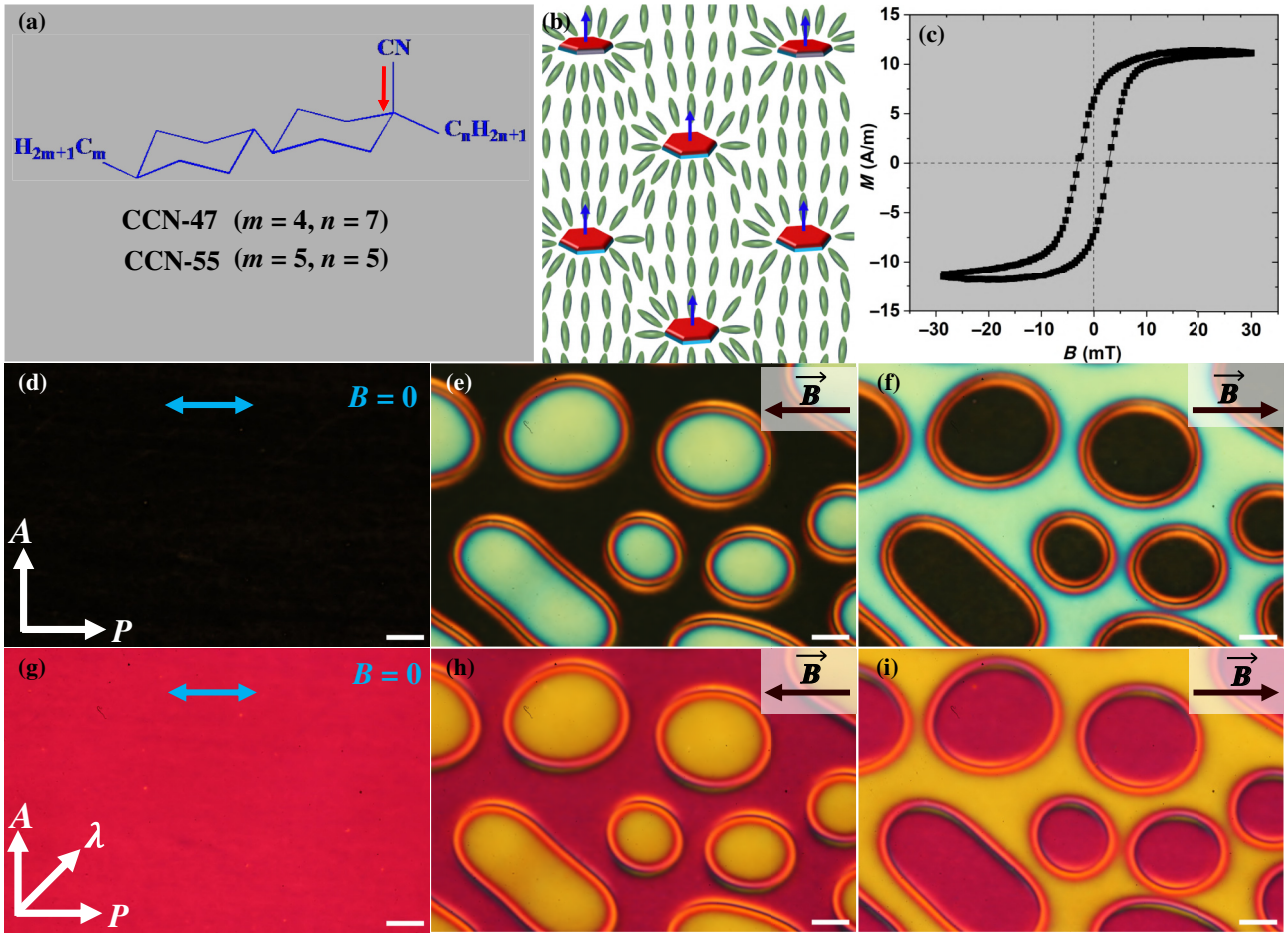

FIG. 1. (a) Molecular structure of CCN-*mn* (cyanobicyclohexane liquid crystals) compounds. (b) Schematic diagram showing the orientation of the magnetic moments of the nanoplatelets and the director in a uniform nematic liquid crystal. (c) Magnetization versus magnetic field of the suspension (1.2 wt % barium hexaferrite in CCN mixture). (d) Polarizing optical microscope (POM) image under crossed polarizers and at zero magnetic field. (e),(f) POM images with an 80-mT magnetic field applied parallel to the director but in opposite directions. (g)–(i) Corresponding images with the retardation plate (λ plate, 530 nm). The director in the bright domains is twisted throughout the cell gap. Cell gap = 9.8 μm. Scale bar = 100 μm. Temperature $T = 26\,^{\circ}$C. Double-headed blue arrows indicate the rubbing direction. *A* and *P* represents analyzer and polarizer, respectively.

dispersing barium hexaferrite (BaHF) nanoplatelets in a bicyclohexene liquid crystal with a transverse -CN group that exhibits a large negative dielectric anisotropy and small birefringence. We study the effect of magnetic field on the alignment, dielectric permittivity, birefringence, and shear viscosity. We show that the prepared ferromagnetic nematic displays profound magnetocapacitance and magnetoviscosity effects. Further, large simultaneous magnetic and electric fields decouple and reorient the nanomagnets orthogonal to the director.

II. EXPERIMENT

A. Preparation of ferromagnetic nematic suspension

We synthesized scandium-substituted BaHF nanoplatelets with nominal composition $BaFe_{11.5}Sc_{0.5}O_{19}$ using a hydrothermal method [4,19,20]. The nanoplatelets have a thickness of approximately 5 nm, and the diameter distribution is approximately log-normal, with a mean of 60 nm and a standard deviation of 20 nm. The nanoplatelets were functionalized with dodecylbenzenesulphonic acid (DBSA) in 1-butanol. The direction of the magnetic moment is perpendicular to the plane of the nanoplatelets. The DBSA functionalization favors the perpendicular orientation (homeotropic) of the nematic director at the nanoplatelet's surface. Hence, the magnetic moment ($\vec{m}$) is parallel to the director $\hat{n}$ [Fig. 1(b)] [4]. The chemical structure of the LCs, *trans*,*trans*-4,4′-dialkyl-(1α,1′α-bicyclohexyl)-4β-carbonitrile (CCN), is shown in Fig. 1(a). The molecules of CCN-47 have a transverse dipole moment of 3.14 D, and in the nematic phase ($T = 30^{\circ}$) it exhibits low birefringence ($\Delta n = 0.033$) and large negative dielectric anisotropy ($\Delta\epsilon = -5.7$) [21–25]. The compounds show the following phase

transitions: CCN-47, Crystal 25.6 °C Smectic-A 28.2 °C Nematic 57.3 °C Isotropic; and CCN-55, Crystal 25 °C Smectic-B 30 °C Nematic 66.4 °C Isotropic [25]. These compounds were mixed in 1 : 1 ratio. The resulting mixture shows the isotropic-nematic transition at $T_{NI} = 62$ °C and exhibits the nematic phase till room temperature [26]. The ferromagnetic nematic suspensions were prepared by adding BaHF dispersion to the LC mixture above the isotropic temperature. The concentration (wt %) of BaHF nanoplatelets in LC was fixed at 1.2 wt % in all the experiments. The suspension was placed in a furnace at 90 °C for 16 h to evaporate the 1-butanol solvent. After the evaporation of the solvent, the remaining suspension was quenched from the isotropic phase to the nematic phase. The suspension was then centrifuged at 10 relative centrifugal force for 20–30 min to remove the aggregated nanoplatelets and used for the experiments.

B. Experimental methods

The suspensions were studied in cells made of indium tin oxide (ITO)-coated glass plates. To obtain planar cells, the ITO plates were spin-coated with polyimide (AL-1254) and cured at 180 °C for 1 h. The cured ITO plates were machine-rubbed unidirectionally and assembled in an antiparallel way. The cell thickness (7–11 μm) was measured using a fiber spectrometer (Ocean Optic, HR-4000). The ferromagnetic nematic samples were filled into the cell in the nematic phase. The alignment of the sample was observed using a polarizing optical microscope (POM) (Nikon, LV100 POL). The birefringence measurements were carried out with the POM using a Berek compensator (U-CTB, Olympus). To observe the effect of an in-plane magnetic field on the texture and to measure the transmission, a lab-made setup was used [Fig. 3(h)]. In this setup, two disc-shaped rare earth strong magnets of strength 0.3 T (neodymium iron boron, Nd-Fe-B) of thickness 5 mm and diameter 20 mm were placed diametrically opposite in a circular track of diameter 40 mm. These magnets were axially magnetized, i.e., one circular flat face was a north pole, the other circular flat face was a south pole. The magnets were rotated simultaneously in the track to rotate the magnetic field direction. The magnetic field at the centre was calibrated using a Gauss meter.

Magnetization measurements were carried out using a physical property measurement system (Dynacool™ PPMS) over a range of magnetic fields from −30 to 30 mT. The magnetoviscosity measurements were made using a rheometer (Anton Paar MCR-501) with a magnetorheological cell. The cell was composed of two parallel plates with a diameter of 20 mm, and the gap between the plates was fixed at 0.2 mm. The bottom plate was fixed, and the top plate was sheared at different shear rates. The sample temperature was maintained using a Peltier temperature controller attached to the bottom plate. The coil that generates the magnetic field was attached below the bottom plate of the rheometer. A magnetic cover was used to prevent a temperature gradient and magnetic field fluctuations in the system. Before the measurement, the sample was presheared at a fixed shear rate 100 s^{-1} for 5 min to remove heterogeneity in the deformation in the quiescent state. The shear viscosity was measured as a function of the magnetic field at a fixed shear rate of 20 s^{-1}. Magnetodielectric measurements were made using an *LCR* meter (Agilent E4980A) by placing the cell between the two plates of the rheometer and varying the magnetic field. In this experiment, only the magnetic field was varied without any shear.

III. RESULTS AND DISCUSSIONS

To begin with, we put the ferromagnetic nematic suspension in a thin capillary tube provided by Quantum Design for magnetic measurements of liquid samples and measured the hysteresis curve [Fig. 1(c)]. The paramagnetic contributions due to the sample container and the liquid crystal were subtracted from the raw data before plotting. The coercivity was about 2.9 mT, and the approximate saturation magnetization was about 11 Am^{-1}. The suspension was put into a planar cell without an external magnetic field for microscopic observations. The POM image of the sample in the absence of any magnetic field is shown in Fig. 1(d). The dark texture and the corresponding image taken with a λ plate [Fig. 1(g)] show that the director $\hat{\mathbf{n}}$ is aligned homogeneously along the rubbing direction. When the magnetic field of 80 mT was applied along the director, two types of domains were observed [Figs. 1(e) and 1(f)]. When the field was applied parallel to the rubbing direction (right to left), some green domains separated by domain walls with dark surroundings were observed. When the direction of the magnetic field was reversed (left to right), the green domains became dark, and the dark surroundings became green. Corresponding λ-plate images of the domains are shown in Figs. 1(h) and 1(i). These suggest two magnetic domains are present in the sample. The magnetization $\vec{M}$ in the black regions is parallel to the magnetic field $\vec{B}$, and in the green domains, $\vec{M}$ is twisted throughout the thickness with respect to the rubbing direction. When the magnetic field direction is reversed, an opposite effect is observed, i.e., the magnetization of the domain switches and, consequently, the domains change color. A schematic diagram of the director in two neighboring domains under zero magnetic field and their responses under the opposite horizontal magnetic field is shown in Fig. 2(a). It may be mentioned that the domains disappear and the texture becomes uniform when the magnetic field is removed and it reappears at the same locations when the magnetic field is switched on.

To see the effect of the out-of-plane magnetic field, a disc-shaped permanent magnet was placed almost above

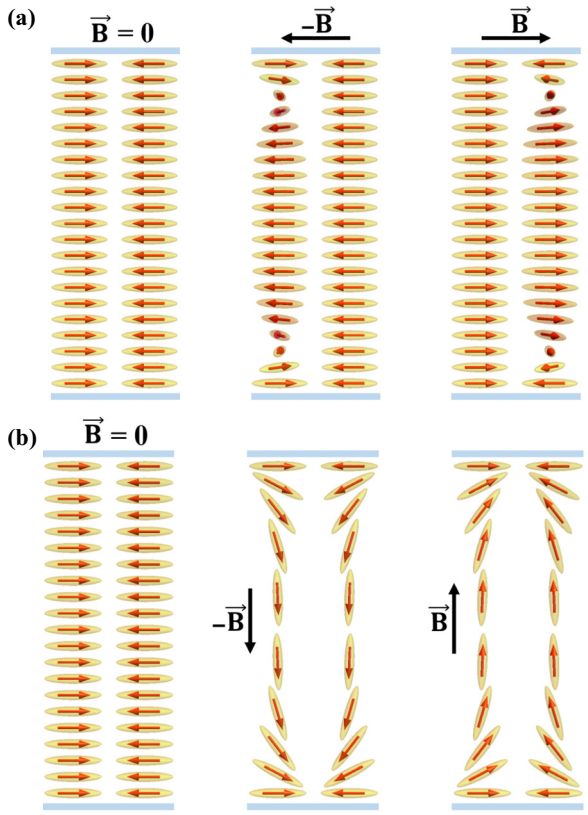

FIG. 2. Schematic diagram of the director in a planar sample with (a) horizontal and (b) vertical magnetic field. Red arrows indicate magnetic dipoles.

the sample near the microscope objective, as shown in Fig. 3(a). In this case, the direction of the magnetic field was nearly perpendicular (approximately 80°). Again, two types of domains separated by domain walls were observed [Fig. 3(b)] and the domain colour did not change when the direction of $\vec{B}$ was reversed [Fig. 3(c)]. However, corresponding λ-plate images show that the domains switched color due to the opposite twist in the two domains [Figs. 3(d) and 3(e)]. Figure 2(b) shows a schematic diagram of the director in neighboring domains under zero magnetic field and their responses under opposite vertical magnetic fields. We can obtain a magnetically monodomain sample with uniform magnetization by applying a magnetic field parallel to the rubbing direction during the cell filling. In this case, the magnetic moments of all the platelets orient in the direction of the magnetic field. Figure 3(f) shows the POM images of a monodomain sample without the magnetic field (rubbing direction oriented at 45°). When the disc magnet was placed above the cell, the magnetic field reoriented the magnetization; hence, the director reoriented towards the magnetic field, and the texture appeared uniformly dark [Fig. 3(g)].

We carried out magneto-optical measurements on a monodomain sample. A planar cell was placed under a polarizing optical microscope, keeping the rubbing direction fixed along the x axis. The transmitted light intensity was measured with the help of a photodiode by rotating the magnetic field 360° stepwise around the cell, as shown schematically in Fig. 3(h). Figure 3(j) shows the polar plot of normalized transmittance at different angles of the magnetic field. It shows two lobes indicating two extinction directions (0° and 180°). Figure 3(i) shows the polar plot of the normalized transmittance without any magnetic field when the microscope stage was rotated by 360°. It has four lobes indicating four extinction directions as expected. This means the director reorients twice when the magnetic field rotates by 360° around the cell. The director's reorientation leads to a moving domain wall, directly observed by the POM. It may be mentioned that the director at the surface remains fixed, while in the bulk, it twists from 0° to an angle that is somewhat lower than 180°, and returns to 0° through a domain reversal. A similar response was reported in ferromagnetic suspensions of 5CB liquid crystal [4].

In what follows, we study the magnetodielectric, birefringence, and magnetoviscosity of the ferromagnetic nematic suspension. Figure 4(a) shows a planar cell's magnetic-field-dependent dielectric constant (ε') when the magnetic field is increased perpendicular to the plane of the cell. At zero magnetic field the effective dielectric constant $\varepsilon'(B=0) \approx \varepsilon'_{\perp} = 10.3$. It decreases rapidly with increasing field and the director finally becomes parallel to the field above 190 mT, where we can consider $\varepsilon'(B = 190\ \text{mT}) \approx \varepsilon'_{\parallel} = 5.9$. Here, the subscript is in reference to the director $\hat{\mathbf{n}}$. From the magnetic-field-dependent dielectric constant, we calculated magnetocapacitance (C_{mag}) using the equation [27,28]

$$C_{\text{mag}} = \frac{\varepsilon(B) - \varepsilon(0)}{\varepsilon(0)} \times 100, \tag{1}$$

where $\varepsilon(B)$ and $\varepsilon(0)$ are the dielectric constants with and without the magnetic field, respectively. The inset of Fig. 4(a) shows a large negative magnetocapacitance ($C_{\text{mag}} \simeq 42\%$) at a small magnetic field. This is much larger than many solid-state composites [28–31]. Hence, these suspensions are promising for magnetoelectric sensors.

Using the Berek compensator, we measured the magnetic-field-dependent birefringence of a planar cell with a magnetically monodomain sample. A lab-made solenoid of radius 25 mm and height 20 mm was placed on the stage of the polarizing optical microscope, as shown in Fig. 4(b). It produces a maximum vertical magnetic field of 20 mT. The cell was placed in the middle of the solenoid. Figure 4(c) shows the variation of birefringence as a function of the applied magnetic field. The birefringence $\Delta n = 0.035$ at zero magnetic field further decreased

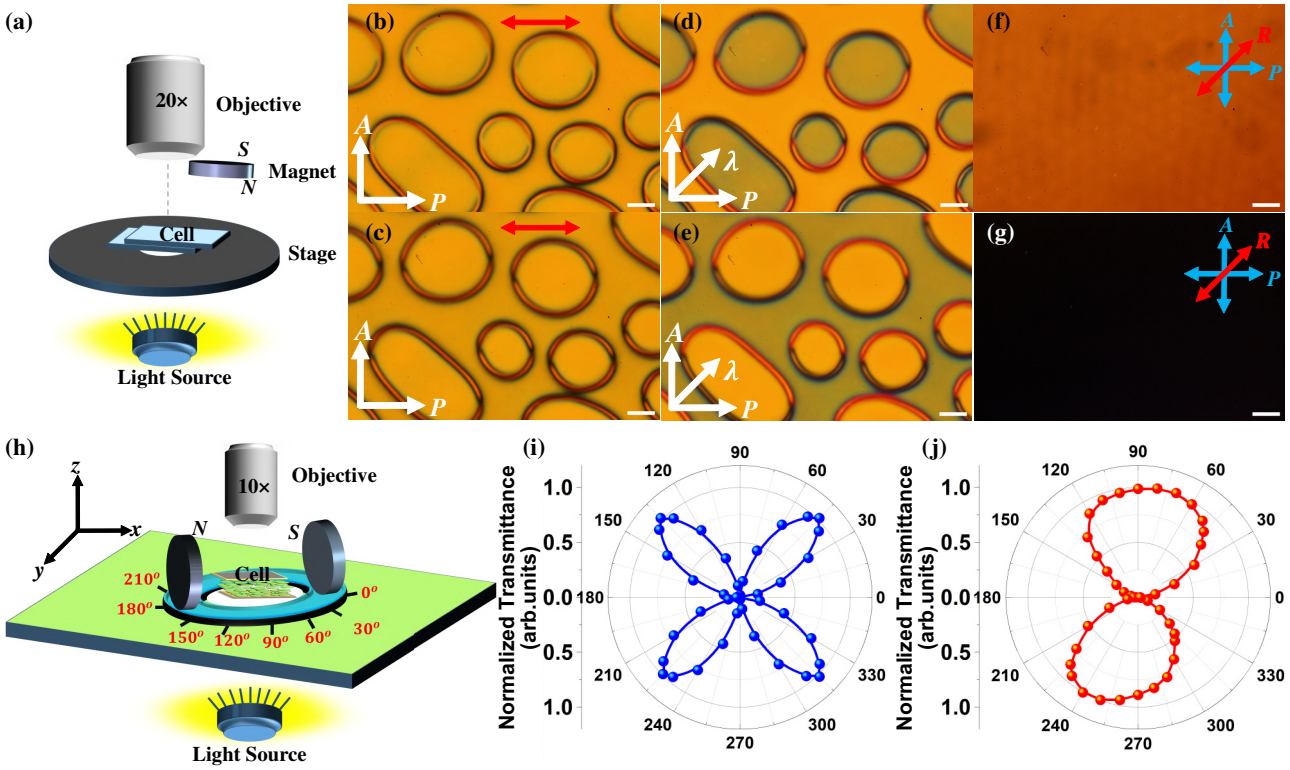

FIG. 3. (a) Schematic arrangement for applying a nearly vertical magnetic field to the cell. A disc-shaped permanent magnet is placed above the cell (near the microscope objective) that produces an 80-mT magnetic field 10° away from the vertical direction. POM images of a polydomain sample (b) when the disc-shaped magnet is placed above the cell and (c) when the magnet is reversed to reverse the magnetic field direction. (d),(e) Corresponding images taken with the λ plate. (f) POM images of a monodomain sample with the director oriented at 45° without any magnetic field. (g) POM image of the monodomain sample with the disc-shaped magnet at the top. (h) Schematic arrangement for applying a rotating magnetic field (20 mT) by moving two diametrically opposite disc-shaped magnets. (i) Normalized transmittance of a monodomain sample when the POM microscope stage with the cell is rotated in the absence of a magnetic field. (j) Normalized transmittance when the magnets are rotated, keeping the cell fixed at the centre and the rubbing direction along the x axis. Cell gap 10 μm. Scale bar = 100 μm. Double-headed orange arrows indicate the rubbing direction.

to 0.018 when the field was increased to 20 mT. This measurement was made up to 20 mT due to the limitation of the maximum magnetic field achievable with the present solenoid.

Like ordinary isotropic ferrofluids [32–34], the viscosity of the ferromagnetic nematic suspensions is influenced by the external magnetic field [13,14,17]. However, due to the inherent anisotropy of the ferromagnetic nematic suspension, the effective viscosity depends on the direction of the magnetic field with respect to the flow direction. We measured the shear viscosity of the ferromagnetic suspension using a magnetorheology setup [14]. The magnetic field was applied perpendicular to the plates. Figure 4(d) shows the effective viscosity η_{eff} of the suspension with increasing and decreasing magnetic field at a fixed shear rate $\dot{\gamma} = 20\ \text{s}^{-1}$. The value of η_{eff} at zero magnetic fields is 144 mPa s, which can be considered as the Miesowicz viscosity η_2, assuming the director is aligned parallel to the shear flow [14]. With increasing magnetic field, η_{eff} increases rapidly and tends to saturate at 345 mPa s above 190 mT. At this field, the director becomes parallel to the magnetic field, hence $\eta_{\text{eff}} \simeq \eta_1$, where η_1 is the Miesowicz viscosity as the director is perpendicular to the shear flow direction. When the magnetic field is reduced, the effective shear viscosity decreases, but the viscosity does not follow the same path. This is attributed to the fact that the sample was initially magnetically multidomain when the forward measurement started, and it transformed into a monodomain sample at a higher magnetic field. However, this transformation is incomplete due to the domain wall pinning and surface imperfections [14].

In general, the magnetic-field-dependent viscosity of a ferrofluid is a nonlinear function and is expressed as $\eta_{\text{eff}} = \eta_0(1 + KH^2)$, where η_0 is the effective viscosity at zero magnetic field and K is the magnetoviscous coefficient. Although the origin of the magnetoviscous effect

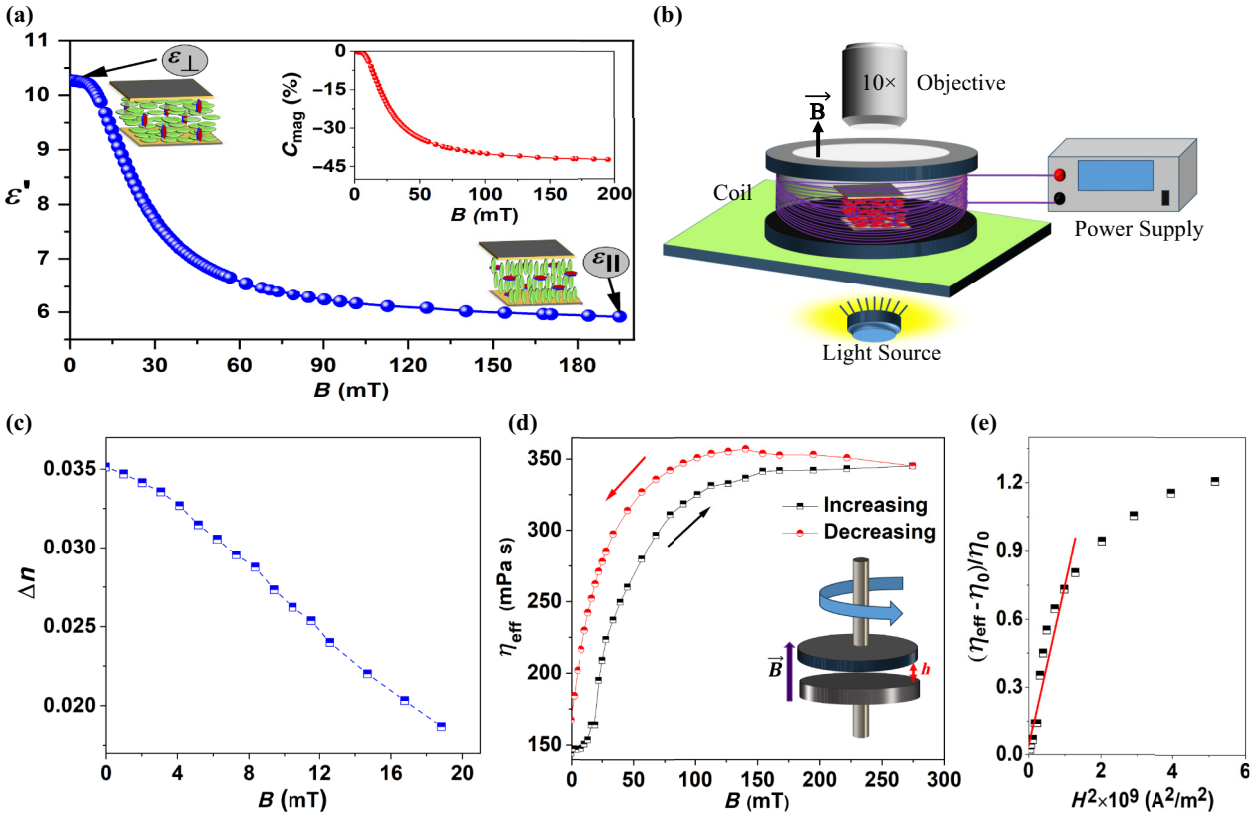

FIG. 4. (a) Real part of the dielectric constant ε' as a function of the magnetic field in a planar cell measured at 4.1 kHz and 0.1 V. The inset shows the magnetocapacitance (MC) as a function of the magnetic field. (b) The schematic diagram for measuring the effect of the transverse magnetic field on the birefringence (Δn). (c) Magnetic-field-dependent birefringence. (d) Effective viscosity η_{eff} as a function of the magnetic field at a fixed shear rate $\dot{\gamma} = 20\,\text{s}^{-1}$. The inset shows the parallel plates with shear and magnetic field directions. Plate gap $h = 0.2$ mm. (e) Variation of $(\eta_{\text{eff}} - \eta_0)/\eta_0$ with H^2. Red lines show a linear fit to Eq. (2). Temperature $T = 26\,^\circ$C.

in isotropic ferrofluids is quite different from that in ferromagnetic nematic suspension, their low magnetic field responses are very similar, i.e., both vary quadratically with the magnetic field. Hence, the linear part of the graph in the low-field region can be expressed as [35]

$$\frac{\eta_{\text{eff}} - \eta_0}{\eta_0} = KH^2. \tag{2}$$

The magnetoviscous coefficient obtained from the fitting is $K = 7.1 \times 10^{-10}$ m^2/A^2 [Fig. 4(e)], which is comparable to many ferrofluids based on a high concentration of particles dispersed in isotropic suspensions [34,35].

Finally, we study the magnetodielectric response at different voltages. In this experiment, the real (ε') and imaginary (ε'') parts of the dielectric constants were measured as a function of the magnetic fields in a planar cell at various voltages using the *LCR* meter. The magnetic field was applied between the two ITO electrodes. In this experiment, at different fixed voltages, the dielectric constant was measured as a function of the magnetic field. Figure 5(a) shows that at 1 V, ε' decreases from 10.3 to 6.2, suggesting the reorientation of the magnetization and the coupled director towards the magnetic field [Fig. 5(d)] compared to the initial state [Fig. 5(c)]. At 2 V, ε' decreases from 10.3 to 8.5, and above 8 V, it becomes almost constant. The imaginary part of the dielectric constant ε'' is shown in Fig. 5(b). It shows that up to 4 V, ε'' increases with the increasing magnetic field and then saturates. At 8 V, the response is different: in particular, ε'' decreases with respect to the zero-field value. With an increasing magnetic field, the magnetic torque increases and tends to reorient the nanomagnets as well as the director towards the magnetic field. At the same time, the dielectric torque tends to keep the director perpendicular to the electric field direction. Since the magnetization and the director are coupled, the magnetic-field-dependent data up to 4 V demonstrate a competing effect of these two torques. Above 8 V, the dielectric torque is so large that the anchoring of the molecules on the nanomagnets is broken. As a result, only the nanomagnets reorient towards the magnetic field, as shown in Fig. 5(e). No

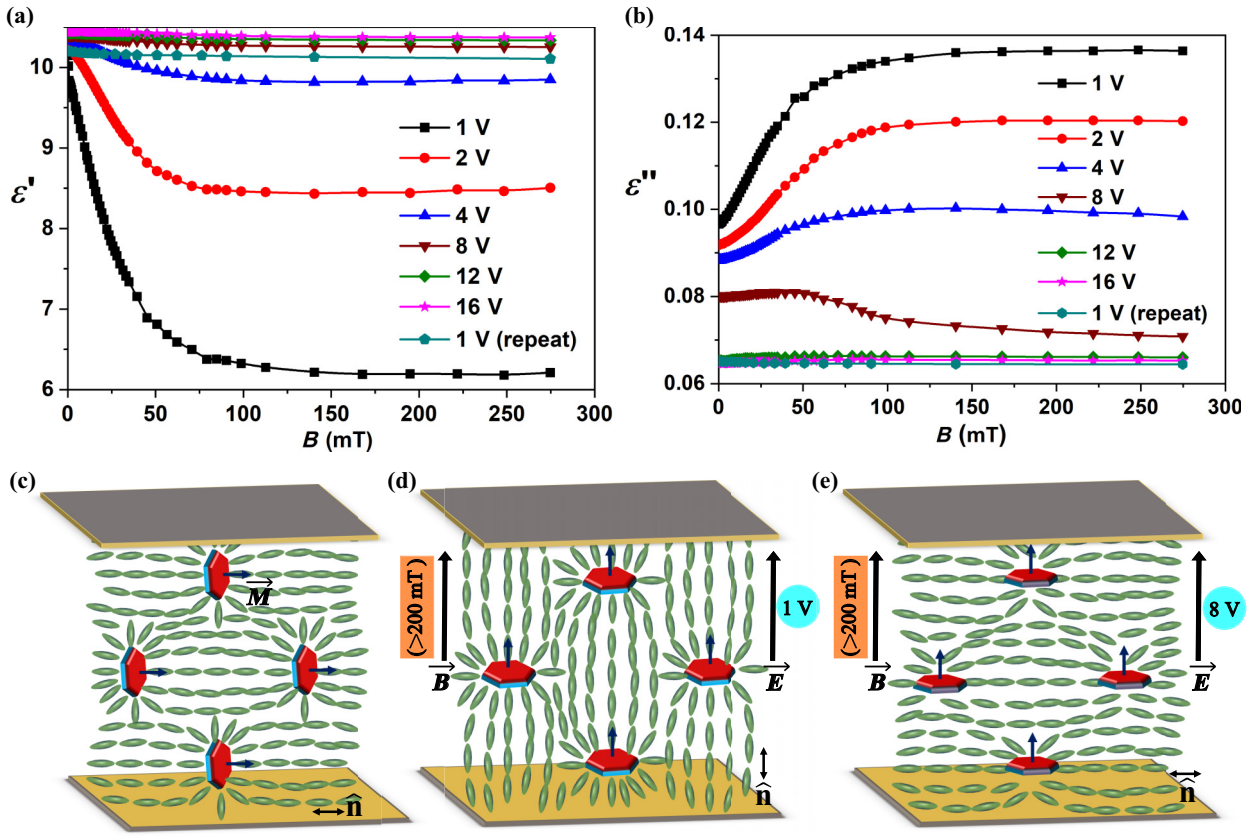

FIG. 5. Variation of (a) the real part ε' and (b) the imaginary part ε'' of the dielectric constant as a function of the magnetic field at a fixed frequency ($f = 4111$ Hz) and various voltages in a planar cell. The magnetic and electric fields were applied in the same direction, perpendicular to the plane of the cell. Schematic diagram showing the orientation of the nanomagnets and the director of a monodomain sample: (c) in the absence of any magnetic or electric fields; (d) at 1 V and $B > 200$ mT; (e) at 8 V and $B > 200$ mT. Cell gap 8.5 μm. Temperature $T = 26$ °C.

further significant changes are observed in ε' and ε'' above 8 V. At the end, the measurement at 1 V was repeated, and the data coincide almost with ε' and ε'' measured at 8 V, which suggests that the perpendicular anchoring of molecules to the platelets is broken permanently. Since $\varepsilon'' = \sigma/\varepsilon_0\omega$, at a fixed frequency, ε'' data reflect the variation of the conductivity of the sample with the magnetic field at different voltages. We believe the decrease of ε'' at 8 V is a pointer to the permanent breaking of the liquid crystal-nanoplatelet anchoring.

Here, two comments are made in order. First, we prepared suspensions at a few other concentrations of the nanoplatelets, but the comprehensive measurements were made only on 1.2 wt%. Second, the viscosity of the fluids depends on the shear rate. Here, the magnetic field and the shear flow have opposite aligning effects, i.e., while the magnetic field tends to reorient the director towards the magnetic field, the high shear rate tends to align it towards the shear flow direction. Our measurements were made at a fixed shear rate of 20 s^{-1} to minimise the effect of strong shear flow.

IV. CONCLUSION

We prepared a ferromagnetic nematic suspension employing a low-birefringence and negative dielectric anisotropy nematic liquid crystal and studied the influence of the magnetic field on magnetic domains and physical properties. We found a large negative magnetocapacitance at a small applied magnetic field. The viscosity increases by 2.4 times due to the reorientation of the director, and the magnetoviscosity coefficient is about 7×10^{-10} m^2/A^2, which is comparable to many isotropic ferrofluids with much larger particle densities than used in the present suspensions. This suspension is useful for applications as a smart fluid, particularly in systems requiring real-time adaptive control or enhanced fluid behavior under specific conditions. The simultaneous magnetic field and electric fields applied perpendicular to the director have antagonistic aligning effects on the nanomagnets and the director in the sense that when the magnetic field is trying to realign the director from the homogeneous to the homeotropic state, the electric field comes into play and tries to restore the homogeneous state. Above a certain

voltage, the perpendicular anchoring of the LC molecules on the nanomagnet is permanently broken, and the magnetic moment of the nanoplatelets and the director orient along mutually orthogonal directions. For device applications requiring simultaneous electric and magnetic fields, the electric field strength should be limited such that it does not decouple the nanoplatelets. This ferromagnetic nematic suspension is useful for fundamental studies such as noncontact manipulation of defects [36], ferrohydrodynamics [37,38], and emerging applications such as magnetic field visualization [39], magnetic field tuning of lasing [15], magnetic switches, etc.

ACKNOWLEDGMENTS

We thank Professor S. Srinath and Jyotiranjan Rout for helping with the magnetization measurements. S.D. acknowledges the support of the PPMS facility of the Institute of Eminence, UoH. S.D. acknowledges financial support from SERB (Grant No. SPR/2022/000001) and the support from the IoE (Grant No. UoH/IoE/RC1-20-010). A.D. acknowledges support from the DST Fellowship (Grant No. DST/WISE-PhD/PM/2023/57). S.S. acknowledges support from an IoE Fellowship, UoH. A.M. and D.L. acknowledge the financial support from the Slovenian Research and Innovation Agency through core funding Grants No. P1-0192 (AM) and No. P2-0089 (DL).

DATA AVAILABILITY

The data that supports the findings of this article cannot be made publicly available. The data are available upon reasonable request from the authors.

[1] P. G. De Gennes and J. Prost, *The Physics of Liquid Crystals* (Clarendon Press, Oxford, U.K., 1993).

[2] P. J. Collings and M. Hird, *Introduction to Liquid Crystals; Chemistry and Physics* (Taylor & Francis Publications, London, 1997).

[3] W. H. de Jeu, *Physical Properties of Liquid Crystalline Materials* (Gordon and Breach Science Publishers, New York, 1980).

[4] A. Mertelj, D. Lisjak, M. Drofenik, and M. Čopič, Ferromagnetism in suspensions of magnetic platelets in liquid crystal, Nature **504**, 237 (2013).

[5] A. Mertelj, N. Osterman, D. Lisjak, and M. Čopič, Magneto-optic and converse magnetoelectric effects in a ferromagnetic liquid crystal, Soft Matter **10**, 9065 (2014).

[6] A. Mertelj, B. Lampret, D. Lisjak, J. Klepp, J. Kohlbrecher, and M. Čopič, Evolution of nematic and ferromagnetic ordering in suspensions of magnetic nanoplatelets, Soft Matter **15**, 5412 (2019).

[7] P. M. Rupnika, D. Lisjaka, M. Čopič, and A. Mertelj, Ferromagnetic liquid crystals for magnetic field visualisation, Liq. Cryst. **42**, 1684 (2015).

[8] Q. Zhang, P. J. Ackerman, Q. Liu, and I. I. Smalyukh, Ferromagnetic switching of knotted vector fields in liquid crystal colloids, Phys. Rev. Lett. **115**, 097802 (2015).

[9] Q. Liu, P. J. Ackerman, T. C. Lubensky, and I. I. Smalyukh, Biaxial ferromagnetic liquid crystal colloids, Proc. Natl. Acad. Sci. **116**, 10479 (2016).

[10] P. M. Rupnika, D. Lisjaka, M. Čopič, S. Čopar, and A. Mertelj, Field-controlled structures in ferromagnetic cholesteric liquid crystals, Sci. Adv. **3**, e1701336 (2017).

[11] N. Sebastián, N. Osterman, D. Lisjak, M. Čopič, and A. Mertelj, Director reorientation dynamics of ferromagnetic nematic liquid crystals, Soft Matter **14**, 7180 (2018).

[12] M. Shuai, A. Klittnick, Y. Shen, G. P. Smith, M. R. Tuchband, C. Zhu, R. G. Petschek, A. Mertelj, D. Lisjak, M. Čopič, J. E. Maclennan, M. A. Glaser, and N. A. Clark, Spontaneous liquid crystal and ferromagnetic ordering of colloidal magnetic nanoplates, Nat. Commun. **7**, 10394 (2016).

[13] T. Potisk, A. Mertelj, N. Sebastián, D. Lisjak, N. Osterman, H. R. Brand, H. Pleiner, and D. Svenšek, Magneto-optic dynamics in a ferromagnetic nematic liquid crystal, Phys. Rev. E **97**, 012701 (2018).

[14] R. Sahoo, M. V. Rasna, D. Lisjak, A. Mertelj, and Surajit Dhara, Magnetodielectric and magnetoviscosity response of a ferromagnetic liquid crystal at low magnetic fields, Appl. Phys. Lett. **106**, 161905 (2015).

[15] M. Mur, J. A. Sofi, I. Kvasic, A. Mertelji, D. Lisjak, V. Niranjan, I. Muševič, and Surajit Dhara, Magnetic-field tuning of whispering gallery mode lasing from ferromagnetic nematic liquid crystal microdroplets, Opt. Exp. **25**, 1073 (2017).

[16] T. Naruta, T. Akita, Y. Uchida, D. Lisjak, A. Mertelj, and N. Nishiyama, Magnetically controllable random laser in ferromagnetic nematic liquid crystals, Opt. Exp. **27**, 24426 (2019).

[17] T. Potisk, D. Svenšek, H. R. Brand, H. Pleiner, D. Lisjak, N. Osterman, and A. Mertelj, Dynamic magneto-optic coupling in a ferromagnetic nematic liquid crystal, Phys. Rev. Lett. **119**, 097802 (2017).

[18] A. Mertelj and D. Lisjak, Ferromagnetic nematic liquid crystals, Liq. Cryt. Rev. **5**, 1 (2017).

[19] D. Lisjak and M. Drofenik, Chemical substitution—An alternative strategy for controlling the particle size of barium ferrite, Cryst. Growth. Des. **12**, 5174 (2012).

[20] P. H. Boštjančič, M. Tomšič, D. Lisjak, and A. Mertelj, Electrostatic interactions between barium hexaferrite nanoplatelets in alcohol suspensions, J. Phys. Chem. C **123**, 23272 (2019).

[21] S. Dhara and N. V. Madhusudana, Influence of director fluctuations on the electric-field phase diagrams of nematic liquid crystals, Eur. Phys. Lett. **67**, 411 (2004).

[22] L. Walz, W. Haase, and R. Eidenschink, The crystal and molecular structures of four homologous, mesogenic *trans*,*trans*-4,4′-dialkyl-(1α,1′α-bicyclohexyl)-4β-carbonitrile (CCNs), Mol. Cryst. Liq. Cryst. **168**, 169 (1989).

[23] S. Dhara and N. V. Madhusudana, Physical characterisation of 4′-butyl-4-heptyl-bicyclohexyl-4-carbonitrile, Phas. Trans. **18**, 561 (2008).

[24] D. Ganzke, S. Wrobel, and W. Haase, Dielectric studies of bicyclohexylcarbonitrile nematogens with large negative

dielectric anisotropy, Mol. Cryst. Liq. Cryst. **409**, 323 (2004).
[25] D. Venkata Sai, T. Arun Kumar, Arun Roy, W. Haase, and S. Dhara, Effect of smectic short-range order on the discontinuous anchoring transition in nematic liquid crystals, J. Chem. Phys. **141**, 044706 (2014).
[26] M. V. Rasna, K. P. Zuhail, R. Manda, P. Paik, W. Haase, and S. Dhara, Discontinuous anchoring transition and photothermal switching in composites of liquid crystals and conducting polymer nanofibers, Phys. Rev. E **89**, 052503 (2014).
[27] G. Catalan, Magnetocapacitance without magnetoelectric coupling, Appl. Phys. Lett. **88**, 102902 (2006).
[28] S. Pachari, S. K. Pratihar, and B. B. Nayak, Enhanced magneto-capacitance response in $BaTiO_3$–ferrite composite systems, RSC Adv. **5**, 105609 (2015).
[29] L. Hrib, L. Pintilie, and M. Alexene, Magnetocapacitance in $La_{0.7}Sr_{0.3}MnO_3/Pb(Zr_{0.2}Ti_{0.8})O_3/La_{0.7}Sr_{0.3}MnO_3$ multiferroic heterostructures, Sci. Rep. **7**, 6563 (2017).
[30] N. S. Rogado, J. Li, A. W. Sleight, and M. A. Subramanian, Magnetocapacitance and magnetoresistance near room temperature in a ferromagnetic semiconductor: La_2NiMnO_6, Adv. Mater. **17**, 2225 (2005).
[31] S. D. Kaushik, S. Rayaprol, J. Saha, N. Mohapatra, V. Siruguri, P. D. Babu, and S. Patnaik, Magnetocapacitance in Ca_3CoMnO_6, J. Appl. Phys. **109**, 07D734 (2011).
[32] J. P. McTague, Magnetoviscosity of magnetic colloids, J. Chem. Phys. **51**, 133 (1969).
[33] S. Odenbach, *Magnetoviscous Effects in Ferrofluids*, Lecture Notes in Physics Monographs (Springer, Berlin, 2002).
[34] S. Odenbach, Ed., *Ferrofluids*, Lecture Notes in Physics, Vol. 594 (Springer, Berlin, 2002).
[35] L. M. Pérez, J. Bragard, P. Díaz, H. L. Mancini, D. Laroze, and H. Pleiner, Magneto-viscous effect on thermal convection thresholds in an Oldroyd magnetic fluid, J. Magn. Magn. Mater. **444**, 432 (2017).
[36] A. J. Hess, Q. Liu, and I. I. Smalyukh, Optical patterning of magnetic domains and defects in ferromagnetic liquid crystal colloids, Appl. Phys. Lett. **107**, 071906 (2015).
[37] R. E. Rosensweig, *Ferrohydrodynamics* (Dover Publications, Mineola, 1997).
[38] S. Odenbach, *Colloidal Magnetic Fluids: Basics, Development and Application of Ferrofluids* (Springer, Berlin, Heidelberg, 2009).
[39] P. M. Rupnik, D. Lisjak, M. Čopičč, and A. Mertelj, Ferromagnetic liquid crystals for magnetic field visualisation, Liq. Cryst. **42**, 1688 (2015).